R*esearch in*
A*stronomy and*
A*strophysics*

Multiple cycles of magnetic activity in the Sun and Sun-like stars and their evolution

Elena Aleksandrovna Bruevich, Vasily Vladimirovich Bruevich and Boris Pavlovich Artamonov

Lomonosov Moscow State University, Sternberg Astronomical Institute, Universitetsky pr., 13, Moscow 119992, Russia; *red-field@yandex.ru; brouev@sai.msu.ru; artamon@sai.msu.ru*

Abstract The wavelet transform method for high-quality time-frequency analysis is applied to sets of observations of relative sunspot numbers and stellar chromosphere fluxes of 10 Sun-like stars. Wavelet analysis of solar data shows that in a certain interval of time there are several cycles of activity with periods of duration which vary considerably from each other: from quasi-biennial cycles to 100-yr cycles. Cyclic activity was detected in almost all Sun-like stars that we examined, even those that previously were not considered as stars with cyclic activity according to analysis using a Scargle periodogram. The durations of solar and stellar cycles significantly change during the observation period.

Key words: Sun: activity — multiple cycles — Sun-like stars: activity

1 INTRODUCTION

The study of cyclic activity, which results from the joint action of electromagnetic and hydrodynamic processes in the interior of the Sun or stars, is a fundamental problem in physics of the Sun and Sun-like stars.

The study of cyclic activity in the Sun began with observations of sunspots. The direct observations of relative sunspot numbers (SSNs) have continued for almost two hundred years. The advantage of SSN index is the fact that data on their annual variations are available from the 1700s: during 1700–1849 they were based on indirect data, then later starting in 1850 direct observations became available. The SSN is a value that measures the number of sunspots and groups of sunspots present on the surface of the Sun.

Sunspots are temporary phenomena on the photosphere of the Sun that are visible as dark spots compared to surrounding regions. They are caused by intense magnetic activity, which inhibits convection by an effect comparable to an eddy current brake, forming areas of reduced surface temperature. Although they have temperatures of roughly 3000–4500 K, the contrast with the surrounding material at about 5780 K makes them clearly visible as dark spots.

The historical sunspot record was first compiled by Wolf in the 1850s and has continued into the 20th century until today. Almost all solar indices and solar wind quantities show a close relationship with the SSN (Svalgaard et al. 2011).

The category of Sun-like stars includes approximately 10% of all stars. Phenomena which are usually called starspots have been observed indirectly for many years, see for example Vaughan & Preston (1980). The main characteristic describing the variations in a star's photospheric radiation is the spottiness of the star. The study of the relative SSNs on the Sun and spotting on stars is very important for explaining the analog observations of Sun-like stars. Activity in the atmospheres of Sun-like stars, such as their photospheric and coronal activity, correlates well with the fluxes in emission lines of H and K of CaII. We have shown that there exists a close interconnection between photospheric and coronal flux variations for the Sun and Sun-like stars in late spectral classes, between radiation fluxes which characterize the energy release from different atmospheric layers,

see Bruevich & Alekseev (2007); Bruevich et al. (2001, 2014).

The aim of our paper is a time-frequency analysis of sets of observations of relative SSNs and observations of stellar chromosphere fluxes by using the method of wavelet transform. We also want to emphasize the similarity of cyclic activity in the Sun and Sun-like stars, which is reflected in the fact that (a) multiple cycles exist at the same time; (b) the periods of these cycles are not constant, and they gradually decrease from their maximum to their minimum value. There comes a moment when this cycle abruptly changes the minimum value of its period up to the maximum value of its period. Then a new gradual decrease starts in the cycle's period over time.

2 WAVELET-ANALYSIS OF A SERIES OF OBSERVATIONS OF SSN WITH DAUBECHIES MOTHER WAVELETS

As manifestations of increased magnetic activity, sunspots indicate different phenomena of solar activity such as coronal loops, prominences and reconnection events. Most solar flares and coronal mass ejections originate in magnetically active regions around visible sunspot groupings. Thus cyclic variations of the SSN and the evolution of these cycles in time is an important task for the study of all complex phenomena on the Sun associated with different indices of solar activity.

The main task of time-frequency analysis is to extract an informative low-frequency component of the time series and screen out the irregular noise of high-frequency components (it is known that useful information is located in the low-frequency region of the signal spectrum and interference or noise is in high frequency).

When digitally processing a signal, a certain transformation is usually applied to reveal the characteristic features of this signal. Then certain actions are performed (for example, the noise suppression), and subsequently it is possible do an inverse transformation. A classic example is the Fourier transform, which transforms the signal from the time domain to the frequency domain and back. The wavelet transform of the temporal signal also makes it possible do the inverse transformation with high accuracy.

First we study the yearly averaged values of SSNs, a data set spanning three hundred years, which we display in Figure 1(a).

We use data from the National Geophysical Data Center website available at *http://www.ngdc.noaa. gov/stp* (Solar Data Service (2018)). These observations allow us to examine cyclical solar activity on a long timescale, up to a century.

In Figure 1(a) we can see that the duration of the main activity cycle, the 11 yr cycle, ranges mainly from 9 to 13 yr. The results become more accurate at the beginning of direct solar observations (1850–2015).

In Figure 1(b) we can see the Fast Fourier Transform (FFT) results for the study of variations in sunspot activity (SSN) over the last 300 yr. We can see that the precise peak in the strongest frequency corresponds to 10.83 yr. If we extend the X axis to 150 yr, we will also see two large, but very wide (due to a temporary change in the values of periods), peaks which are centered on the time interval of about 50 yr and 100 yr.

The Fourier transform (traditionally used for time series analysis) has the following main limitations: it does not distinguish a signal that is the sum of two sinusoids from the situation of sequential inclusion of sinusoids and does not provide information on the preferential frequency distribution over time.

The wavelet transform differs from traditional time-frequency analysis (Fourier analysis, Scargle's periodogram method) because of its efficient ability to detect and quantify multi-scale, non-stationary processes, see Frick et al. (1997). The wavelet transform maps a one-dimensional time series $f(t)$ into a two-dimensional plane, related to time and frequency scales. Wavelets are the localized functions which are constructed based on one so-called mother wavelet $\psi(t)$. The choice of wavelet is dictated by signal or image characteristics and the nature of the application. Understanding properties of the wavelet analysis and synthesis, you can choose a mother wavelet function that is optimized for your application.

For analysis of time series of astronomical observations, the Morlet and Daubechies mother wavelets are most often used. Obviously, the best result in obtaining information on the magnitude and temporal evolution of the low-frequency signal, which is informative for researchers, will be achieved in the case when the mother wavelet is well correlated with the analyzed signal.

The wavelet coefficients that determine the probability that a periodicity takes place at a particular frequency are calculated by means of the integral temporal convolution of the studied signal with the mother wavelet. Therefore, if the time signal being examined has
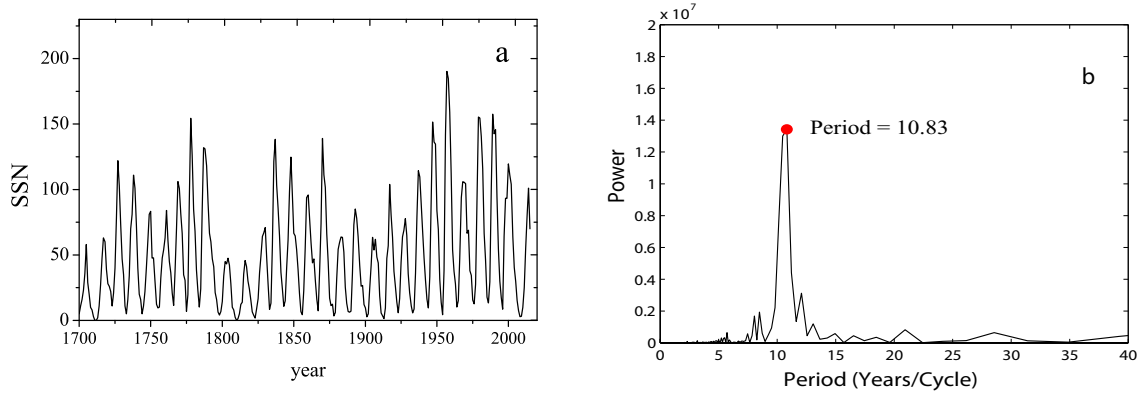
Fig. 1 The relative SSNs: (a) Yearly averaged observations from 1700 to 2015; (b) The FFT of the time series of yearly averaged values of SSNs from 1700 to 2015. The *solid dot* marks the peak of the strongest frequency.

a pseudo-sinusoidal form, the mother wavelet must be constructed using a superposition of several sinusoids.

In addition, the mother wavelet function must include local properties of the signal (rapid increases and rapid declines), which are characteristics of the Dirac delta function (δ-function) that is widely used in signal processing.

The Morlet mother wavelet, which is often used in the analysis of time series of astronomical observations, satisfies these requirements, since the Morlet mother wavelet is a superposition of a plane wave and a δ-function.

Unlike the Morlet wavelet which is given by an analytical expression, the family of Daubechies wavelets of different orders is constructed with the help of polynomial iteration formulas. Ingrid Daubechies in the 1990s developed a collection of wavelets that are remarkably efficient, see Daubechies (1990). The Daubechies wavelet of the lowest order is a Haar wavelet.

The family of Daubechies wavelets refers to orthogonal wavelets with compact support and is calculated in an iterative way. Higher order Daubechies wavelets are successively constructed from lower order Daubechies wavelets. Note that the Daubechies 2 mother wavelet is a polynomial of order 1, and the Daubechies 10 mother wavelet is a polynomial of order 5. The choice of a particular class of mother wavelets is dictated by the specifics of the problem (the information that needs to be extracted from the signal). In a number of cases, with the help of various wavelets, the features of the analyzed signal can be more fully revealed.

The basic properties of Daubechies wavelets are listed below:

(1) The Daubechies wavelet system has smoothness properties. This increases the accuracy in determining the informative frequency of the time series under study. The increase in the smoothness of the Daubechies functions in the frequency domain occurs with an increase in their order.
(2) Daubechies wavelets have properties of compactness (they rapidly increase and fall rapidly) and orthogonality, which makes an accurate recovery of a temporary signal possible;
(3) The property of orthogonality in Daubechies wavelets allows the user to obtain independent information on different scales.

For processing time series of monthly observations of solar activity indices, such as SSN and $F_{10.7}$, we have compared calculations with the help of both the Morlet wavelet and Daubechies wavelet of orders 8–12. Using Daubechies wavelet of orders higher than 10 only complicates the calculations without improving of the quality of the wavelet mapping.

The result of wavelet analysis (Morlet and Daubechies 10 wavelets) applied to a series of observations of yearly SSN is presented in the form of many of isolines, see Figure 2(a) and 2(b). For the same isoline, the values of the wavelet coefficients are of the same. The maximum values of isolines indicate the maximum values of wavelet coefficients, which correspond to the most likely value of the period of the cycle, see the scale bar on the right of each panel. The temporal evolution of the value of the period cycles is determined by the line connecting different maxima, see Figure 2(a).
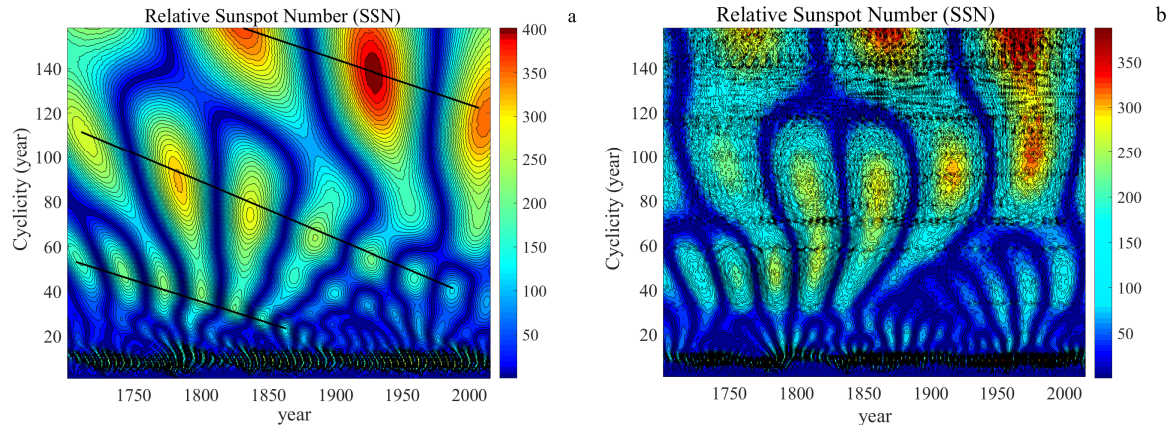
Fig. 2 The wavelet image of the time series of the yearly averaged values for SSN from 1700 to 2015: (a) wavelet transform calculations with the Daubechies 10 mother wavelet; (b) wavelet transform calculations with the Morlet mother wavelet.
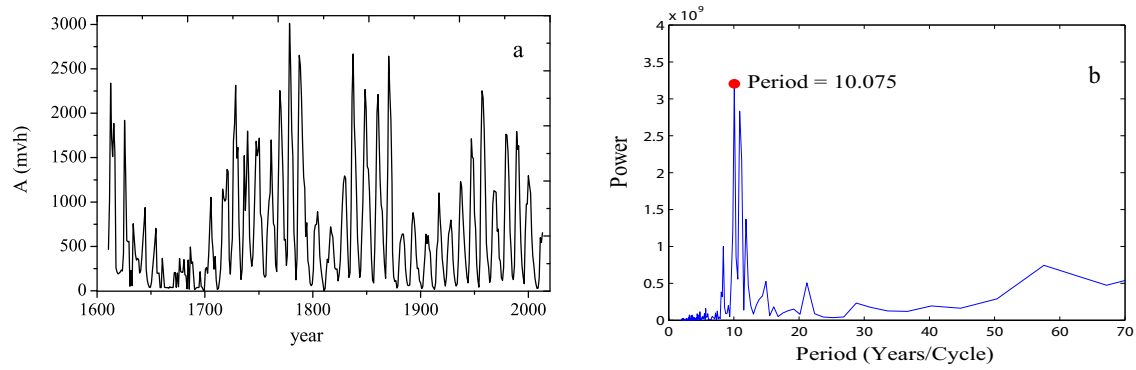

Fig. 3 The areas of SSNs A (mvh-millionth of hemisphere): (a) Yearly averaged observations from 1610 to 2015; (b) The FFT of the time series of the yearly averaged values of the areas of SSNs A (mvh) from 1610 to 2015. The *solid dot* shows the precise peak associated with the strongest frequency.
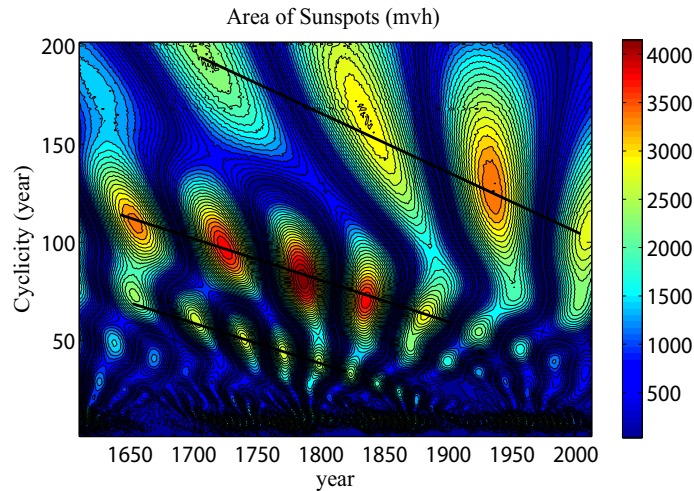

Fig. 4 The wavelet image of the time series of the yearly averaged values of the areas for SSNs A (mvh) from 1610 to 2015 (for wavelet transform calculations, we used the Daubechies 10 mother wavelet). The *dark lines* show temporal trends in cycle duration.

Relative Sunspot Number (SSN)
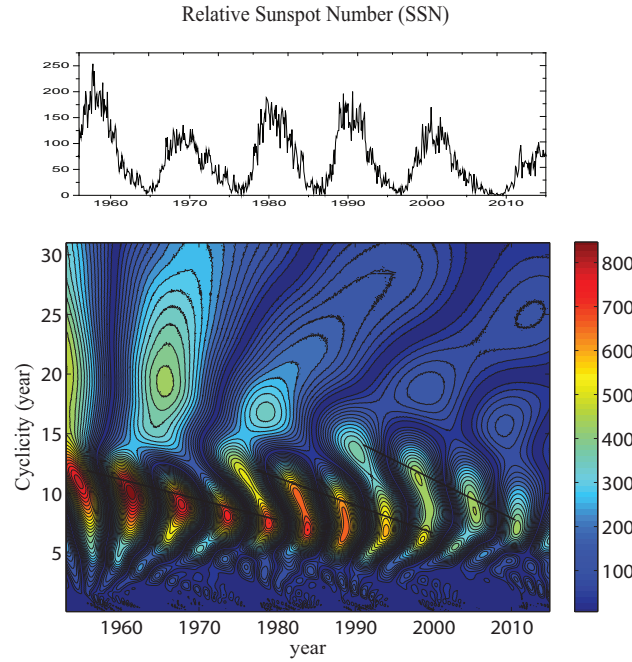
Fig. 5 Monthly averaged relative SSNs during 1950–2015 (*top panel*); Cyclic activity of relative SSNs in activity cycles 18–24 (*bottom panel*). The *dark lines* show temporal trends in the cycle duration.

Relative Suspot Number (SSN)
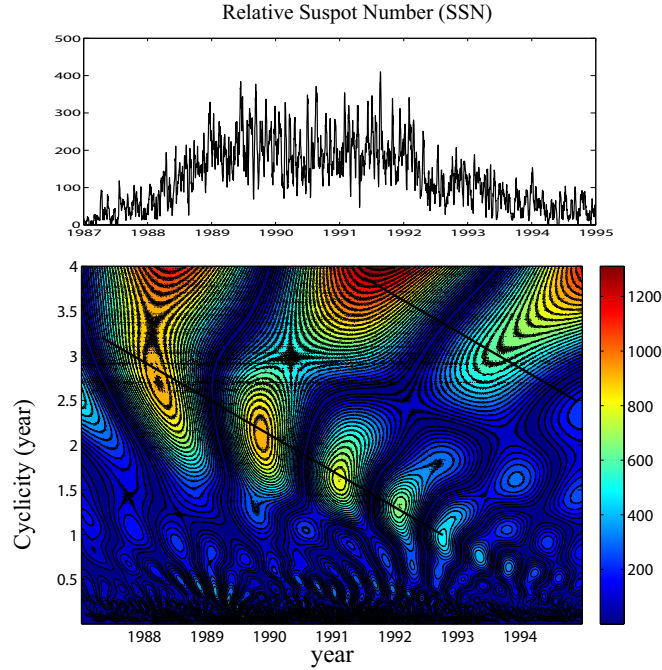
Fig. 6 Daily averaged relative SSNs during 1986–1997 (*top panel*). Cyclic activity of relative SSNs on the quasi-biennial timescale (*bottom panel*). The *dark lines* show temporal trends in the cycle's duration.

In Figure 2(a) and 2(b) we have illustrated, with help from wavelet analysis, the fact that the long term series of observations gives us very useful information to study the problem of solar flux cyclicity on long timescales.

The results of the calculations with Morlet and Daubechies 10 wavelets turned out to be quite similar, and the main informative frequencies and wavelet coefficients proved to be almost identical in magnitude. The difference was manifested in two results:
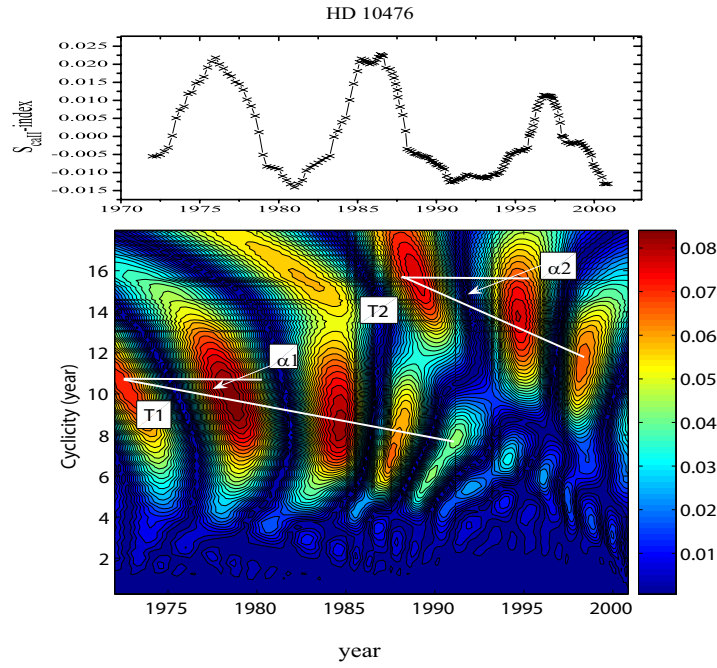
Fig. 7 Three-month averaged data of "Excellent" class star HD 10476. Observations from 1972 to 2002 (*top panel*). Cyclic activity of HD 10476 (*bottom panel*). The *white lines* show temporal trends in the cycle's duration.
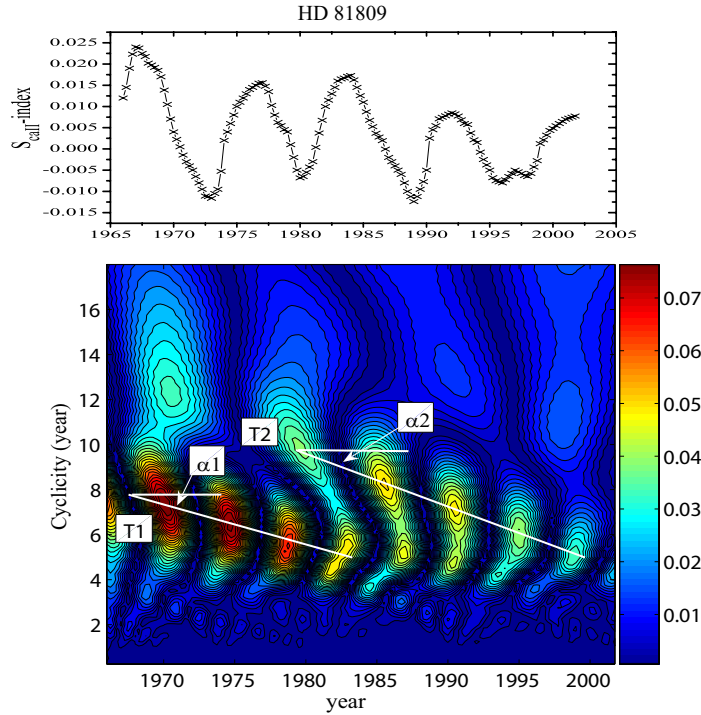
Fig. 8 Three-month averaged data of "Excellent" class star HD 81809. Observations from 1966 to 2002 (*top panel*). Cyclic activity of HD 81809 (*bottom panel*). The *white lines* show temporal trends in the cycle's duration.

(1) The Morlet wavelet maps showed noisier main informative signals than the Daubechies 10 wavelet maps. This is due to the fact that the Daubechies wavelet system has smoothness properties, and these smoothness properties are strengthened with an increase in the order of the Daubechies wavelets. Therefore, for the analysis of astronomical observa-

tions it is recommended to use Daubechies wavelets with orders greater than 8.

(2) In the Morlet wavelet-maps there were no low-frequency components appearing in the Daubechies 10 wavelet-maps. We show these low-frequency components in the form of time trends with solid lines in our figures.

Thus, with the help of Daubechies 10 wavelets, we found (along with the main frequencies of cyclic activity) the existence of long-term trends in the evolution of cyclic periods, which agrees with the results of calculations by Frick et al. (1997) for 100-yr cycles on the Sun and with results of observations of Kolláth & Oláh (2009) for stars.

In Figures 2(a), 2(b) and 4–16, the (X, Y) plane is the time-frequency plane of calculated wavelet coefficients $C(a, b)$: parameter a corresponds to the Y plane (cyclicity, year) and parameter b corresponds to the X plane (time, year). The modules of $C(a, b)$ coefficients, characterizing the probability amplitude of regular cyclic component localization exactly at the point (a, b), are laid along the Z axis. We can see the projection of $C(a, b)$ on the (a, b) or (X, Y) plane. This projection on the plane (a, b) with isolines allows us to trace changes in the coefficients on various scales in time and reveals a picture of local extrema on these surfaces. This is the so-called skeleton of the structure of the analyzed process.

An important index of solar activity is the index of the area of the solar spots, which, in addition to the SSN, is a good indicator of the general level of cyclic activity of the Sun, see Nagovitsyn et al. (2016); Bludova et al. (2014).

In Figure 3(a) we can see that the duration of the main 11-yr cycle of solar activity according to observations of the areas of SSNs A (measured in one millionth of the solar hemisphere – mvh) also ranges mainly from 9 to 13 yr. Here we consider the 400 yr data set of A values from calculations in Nagovitsyn et al. (2016).

In Figure 3(b) we can see the FFT results for the study of variations in the areas of SSNs A over the last 400 yr. We can see that the 300-yr observations (Fig. 1(b)) and the 400-yr observations (Fig. 2(b)) have different peak values for the strongest frequency, which are 10.83 yr and 10.075 yr respectively. This confirms that the frequency of the main cycle of solar activity does not remain constant on timescales of 300 yr and 400 yr.

In Figure 4 we show the wavelet image of the time series of yearly averaged values for the areas of SSNs A (mvh).

In Figure 2 and Figure 4 we see three well-defined cycles of activity: the main cycle of activity (this cycle is approximately equal to 10–11 yr), 40–50 yr cyclicity and 100–120 yr cyclicity. We can also see that periods of cycles on different timescales are not constant: the 50-yr cyclicity changes from 60 to 40 yr and the 100-yr cyclicity changes from 120 to 80 yr.

The long-term behavior of the sunspot group numbers has been analyzed using the wavelet technique in Frick et al. (1997) who plotted the changes in the main Schwabe cycle with a period of about 11-yr and studied the grand minima. The temporal evolution of the Gleissberg cycle (its period is about 100-yr) can also be seen in the time-frequency distribution of solar data. According to Frick et al. (1997), the Gleissberg cycle is as variable as the Schwabe cycle.

For the wavelet analysis of SSN on scales of 11 yr we use the monthly averaged observations, see Figure 5.

A few decades ago, some solar physicists began to examine the variations of relative SSNs with different methods, not only in the high amplitude 11-yr Schwabe cycle but also in low amplitude cycles approximately equal to a half (5.5-yr) and a fourth (quasi-biennial) of the period of the main 11-yr cycle, see Vitinskij et al. (1986). The periods of the quasi-biennial cycles vary considerably within one 11-yr cycle, decreasing from 3.5 to 2 yr, and this fact complicates the study of such periodicity using the method of periodogram estimates.

The quasi-biennial cycles have been studied not only for their relative SSN, but also for 10.7 cm solar radio emission and for some other indices of solar activity through the methods of frequency analysis applied to signals, see Bruevich et al. (2014); Bruevich & Yakunina (2015). It was also shown that the cyclicity on a quasi-biennial timescale takes place often among the stars with stable cyclicity similar to solar 11-yr cycles, see Bruevich & Kononovich (2011).

We can also see that as in the case of the Schwabe cycle the duration of the cycle, which is the period, decreases approximately during three cycles (for the Gleissberg cycle the period of 110 yr decreases to 70 yr – Figure 2 and Figure 4; for the Schwabe cycle the period of 12 yr decreases to 8 yr – Figure 5).

In Figure 6 we can see that in the case of quasi-biennial cycles the behavior of these periods inside the

11-yr cycle is similar to the variation of cycle periods in the Schwabe cycle and the Gleissberg cycle. The periods of quasi-biennial cycles change from 3.5 to 2 yr inside the 11-yr cycle.

In Table 1 below, we denote the 11-year main periodicity for the Sun as period $T1$, centennial periodicity as period $T2$ and quasi-biennial periodicity as period $T3$.

According to *Kepler* observations and *CoRoT* data "shorter" activity cycles with periods of about two years were also found for Sun-like F, G and K stars, see Metcalfe et al. (2010), García et al. (2010).

In Kolláth & Oláh (2009), different methods, such as short-term Fourier transform, wavelet and generalized time-frequency distributions, have been tested and used for analyzing temporal variations on timescales of long-term observational data which have information on the magnetic cycles of active stars and that of the Sun. It was shown that the application of wavelet analysis is preferable when studying a series of observations of the Sun and stars. Their time-frequency analysis of multi-decadal variability in the solar Schwabe (11-yr) and Gleissberg (century) cycles during the last 250 yr indicated that one cycle (Schwabe) varies between limits, while the longer one (Gleissberg) continually increases. By analogy with the analysis of the longer solar record, the presence of a long-term trend may suggest an increasing or decreasing multi-decade cycle that is presently unresolved in stellar records with short duration.

In Figure 6 we show the results of wavelet analysis of daily SSN data in solar cycle 22. We analyzed those data on a timescale which is equal to several years and identified second order periodicity such as 5.5 yr and quasi-biennial as well as their temporal evolution.

In Oláh et al. (2009), it was found that cycles of 20 Sun-like stars show systematic changes. It was also found that 15 stars definitely show multiple cycles, but the records of the other five stars are too short to verify a timescale for a second cycle. The results for six HK-project stars (HD 131156A, HD 131156B, HD 100180, HD 201092, HD 201091 and HD 95735), the same stars from Oláh et al. (2009) and Baliunas et al. (1995), are different.

Cyclicity similar to the solar quasi-biennial case was also detected in Sun-like stars from direct observations. In Morgenthaler et al. (2011), the results of direct observations of magnetic cycles of 19 Sun-like F, G and K type stars spanning 4 yr were presented. Stars in this sample are characterized by masses between 0.6 and 1.4 solar masses and by rotation periods between 3.4 and 43 days. Observations were made using the NARVAL spectropolarimeter (Pic du Midi, France) between 2007 and 2011. It was shown that for the stars τ Boo and HD 78366 in this sample (the same as the Mount Wilson HK-project) the cycle lengths derived by Baliunas et al. (1995) seem to be longer than those derived by spectropolarimetry observations of Morgenthaler et al. (2011). They suggest that this apparent discrepancy may be due to the different temporal samplings inherent to these two approaches, so that the sampling adopted at Mount Wilson may not be sufficiently tight to unveil short activity cycles. They hope that future observations of the Pic du Midi stellar sample will allow them to investigate longer timescales of the stellar magnetic evolution.

Using methods of frequency analysis for signals, quasi-biennial cycles have been studied not only with relative SSN, but also with 10.7 cm solar radio emission and some other indices related to solar activity, see Bruevich & Yakunina (2015). It was also shown that cyclicity of the quasi-biennial timescale often takes place among stars with 11-yr cyclicity, see Bruevich & Kononovich (2011).

We assume that precisely these quasi-biennial cycles were identified in Morgenthaler et al. (2011): τ Boo and HD 78366 are the same stars as in the HK-project; these stars have cycles similar to the quasi-biennial solar cycles with periods of a quarter of the duration of the periods defined in Baliunas et al. (1995).

Note that in the case of the Sun, the amplitude of variations of the radiation in quasi-biennial cycles is substantially less than the amplitude of variations in main 11-yr cycles. We believe that this fact is also true for all Sun-like stars in the HK-project and in the same way for τ Boo and HD 78366.

The quasi-biennial cycles cannot be detected with Scargle's periodogram method. However, methods of spectropolarimetry from Morgenthaler et al. (2011) allowed detecting cycles with 2 and 3-yr periods. Thus, spectropolarimetry is a more accurate method for detection of cycles with different periods and with low amplitudes of variation.

So, the need to apply wavelet analysis to HK-project observational data is dictated also by the fact that application of the wavelet method to these observations will help: (1) to find cyclicities with periods equal to a half and a quarter of the main high amplitude cyclicity; (2) to clarify periods of high amplitude cycles and to follow
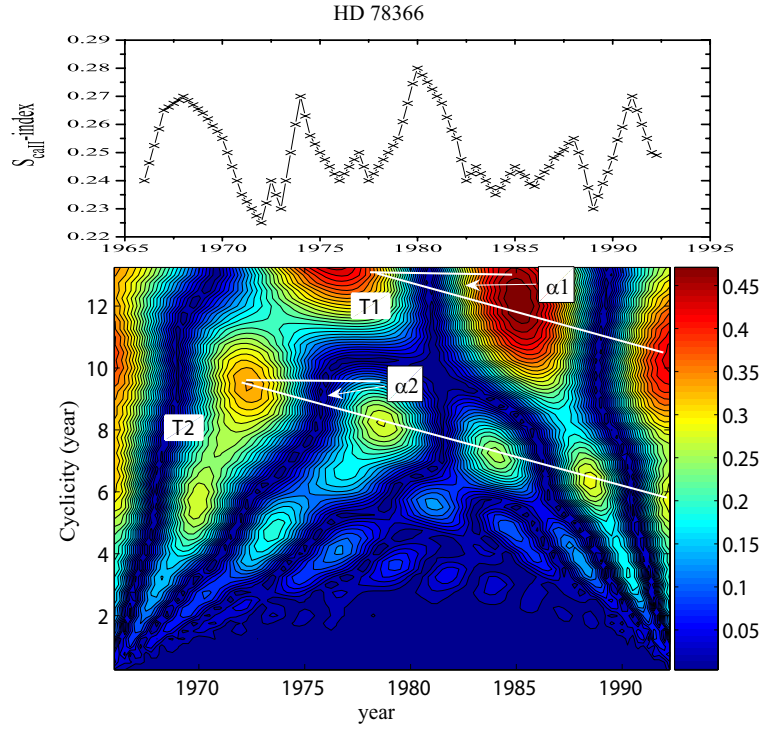
Fig. 9 Three-month averaged data of "Good" class star HD 78366. Observations from 1966 to 1993 (*top panel*); Cyclic activity of HD 78366 (*bottom panel*). The *white lines* show temporal trends in the cycle's duration.
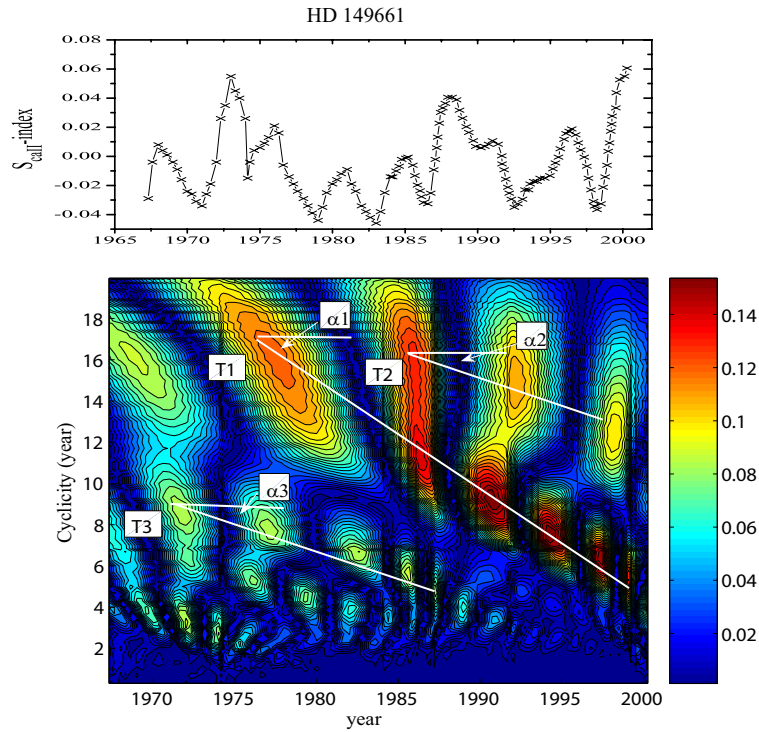
Fig. 10 Three-month averaged data of "Good" class star HD 149661. Observations from 1966 to 2001 (*top panel*); Cyclic activity of HD 149661 (*bottom panel*). The *white lines* show temporal trends in the cycle's duration.

Table 1 Parameters Associated with Different Cycles

HD	Class	$T1^0$ (yr)	$t1^0$ (yr)	$\alpha1$	$T2^0$(yr)	$t2^0$ (yr)	$\alpha2$	$T3^0$ (yr)	$t3^0$ (yr)	$\alpha3$
Sun	Excl	11.5	1955.0	20°	105	1970.0	22°	3.0	1988	25°
81809	Excl	8.0	1967.5	16°	9.7	1980.5	22°	–	–	–
10476	Excl	10.7	1972.0	12°	15.5	1988.0	26°	–	–	–
78366	Good	13.0	1976.0	16°	9.2	1972.0	17°	–	–	–
149661	Good	17.2	1977.0	33°	16.5	1987.0	18°	9.0	1972	19°
1835	Fair	22.0	1982.5	12°	11.2	1976.0	16°	–	–	–
18256	Fair	17.5	1982.5	28°	7.2	1969.0	13°	11.0	1984	29°
35296	Long	22.0	1982.5	15°	14.0	1974.0	21°	–	–	–
143761	Long	19.7	1982.5	30°	9.6	1966.0	28°	–	–	–
13421	Flat	18.5	1977.5	18°	6.2	1966.0	16°	8.0	1991	22°
39587	Var	22.5	1985.5	10°	16.0	1966.5	22°	16.5	1975	17°

their evolution in time; (3) to find other stars with cycles that were not determined using the periodogram method.

3 MAGNETIC CYCLES OF HK PROJECT STARS. OBSERVATIONS AND WAVELET ANALYSIS

In this paper, the time series of observations of 10 stars from the HK project are studied. We used observations of the CaII H&K emission (the Mount Wilson S – index (S_{HK}) is the ratio of the core of the CaII H&K lines to the nearby continuum) which is established now as the most sensitive indicator of chromospheric activity in lower main sequence stars, see Vaughan & Preston (1980), Zhao et al. (2015).

All stars in the HK project were carefully chosen according to physical parameters, which are closest to the Sun: cold, single stars – dwarfs, belonging to the main sequence. Binary systems are excluded, see Shimanovskaya et al. (2016).

Results of combined observations of radiation fluxes of the HK project and rotational modulation of observed fluxes (Noyes et al. 1984) show the existence of surface heterogeneity in stars that live and develop during several periods of rotation around their axes. In addition, evolution of the periods of rotation for stars in time clearly indicates the existence of a star's differential rotation, similar to the Sun's differential rotation.

The record of solar chromospheric variations is an important point for comparison with stellar activity records. In Baliunas et al. (1995), the 10.7 cm solar radio flux data were converted to star records in the HK project (S-index).

HK project stars were determined to be different stellar classes according to results of calculations of power spectra from the time series. It was assumed that the time series were "Excellent," "Good" and "Fair." It was shown that the duration of the cycles varies from 7 to 20 years for different stars and stars with cycles represent about 30% of the total number of studied stars. The classification of stars without cycles consists of "Var" (significant variability with no clear period from the power spectrum analysis), "Flat" (no significant variability) and "Long" (variability on timescales longer than about 20 yr).

In our paper we have applied wavelet analysis for partially available data from the records of relative CaII emission fluxes – the variation of S_{HK} for 1965–1992 observations from Baliunas et al. (1995) and for 1985–2002 observations from Lockwood et al. (2007). We used the detailed plots of S_{HK} time dependencies: each point represents a record from observations, which we processed in this paper using the wavelet analysis technique, corresponding to 3 months of averaged values for S_{HK}.

We have studied 10 HK-project stars: with cyclic activity in the "Excellent" class – HD 10476 and HD 81809, with cyclic activity in the "Good" class – HD 78366 and HD 149661, with cyclic activity in the "Fair" class – HD 1835 and HD 18256, stars in the "Long" class – HD 35296 and HD 143761, a star in the "Flat" class – HD 13421 and a star in the "Var" class – HD 39587.

We used the Daubechies 10 wavelet technique which can most accurately determine the dominant cyclicity as well as its evolution in time in solar data sets at different wavelengths and spectral intervals (Bruevich & Yakunina 2015).

We hope that wavelet analysis can be used to help study the temporal evolution of chromospheric activity

cycles in the stars. Three-month averaging also helps us to avoid the modulation of observational S_{HK} data from stellar rotations.

3.1 HK Project Stars in the "Excellent" Class

In Baliunas et al. (1995) and Lockwood et al. (2007) the regular chromospheric cyclical activity of HK-project Sun-like stars was studied through analysis of the power spectral density with Scargle's periodogram method. Baliunas et al. (1995) computed the Scargle's periodogram for all the 111 stars in that study. The significance of the height of the tallest peak in the periodogram was estimated by the false alarm probability (FAP) function (expressed in percent), see Scargle (1982).

We use the combined data sets from Baliunas et al. (1995) and from Lockwood et al. (2007) for stars in the "Excellent" class – HD 10476 and HD 81809. In Shimanovskaya et al. (2016) we have analyzed these stars by applying the Complex Morlet mother wavelet and confirmed the Baliunas et al. (1995) determination of periods. We have also shown that HD 10476 changed its period after 1988; the period of the cycle changed sharply from 8.2 to 13.5 yr.

We denoted the most probable period (determined from the array of wavelet coefficients according to the scale on the right side of the picture) as $T1$, and the weaker periods (if they were determined from the analysis) were denoted as $T2$ and $T3$.

In Figure 7 we demonstrate the advantages of the Daubechies 10 wavelet in the case when we want to investigate the time evolution of cycles. For HD 10476 we see that the main cycle of the "Excellent" class ($T1$) is not constant (9.6 yr according to Baliunas et al. (1995)) but changes from 11 to 8 yr from 1972 to 1990. Simultaneously with this cycle ($T1$), there is another cycle ($T2$) with a larger period which changed from 15.5 yr to 12 yr from 1985 to 2002. We see that in 1984–1992 there are two significant periods, $T1$ and $T2$. Although the Morlet wavelet shows an abrupt change in 1985, an analysis with a Daubechies wavelet shows that there is a splitting of the periodicity into two components.

In Figure 8 we show the cycle changing for HD 81809. We have also analyzed stars in Shimanovskaya et al. (2016) with the Complex Morlet wavelet and confirmed Baliunas et al. (1995)'s period ($T1 = 8.17$ yr). An analysis with a Daubechies wavelet shows that $T1$ changes from 8 to 5 yr in 1966–1985 and

simultaneously there exists another weaker cycle $T2$ which changed from 10 to 5.6 yr in 1980–2002.

3.2 HK Project Stars in the "Good" Class

We use the combined data sets from Baliunas et al. (1995) and Lockwood et al. (2007) for stars in the "Good" class – HD 78366 and HD 149661.

In Figure 9 we show the results of our calculations of "Good" class star – HD 78366. We can see that the main period (12.2 yr according to Baliunas et al. (1995)) changed from 13 yr to 11 yr in 1973–1993. We can also see that there simultaneously exists another weaker cycle $T2$ which changed from 9.5 to 6 yr from 1972 to 1993.

In Figure 10 we show the results of our calculations of "Good" class star – HD 149661. We see three cycles for this star. The main period $T1$ (17.4 yr according to Baliunas et al. (1995)) is reduced from 18 to 6 yr from 1977 to 2000. The significant period $T2$ is reduced from 16 to 13 yr from 1987 to 1998. The superposition of these periods $T1+T2$ likely yields a value of 17.4 years, as calculated in Baliunas et al. (1995). In Figure 10 we can also see another weaker cycle with a period of $T3$ which changed from 9 yr to 5 yr from 1972 to 1987.
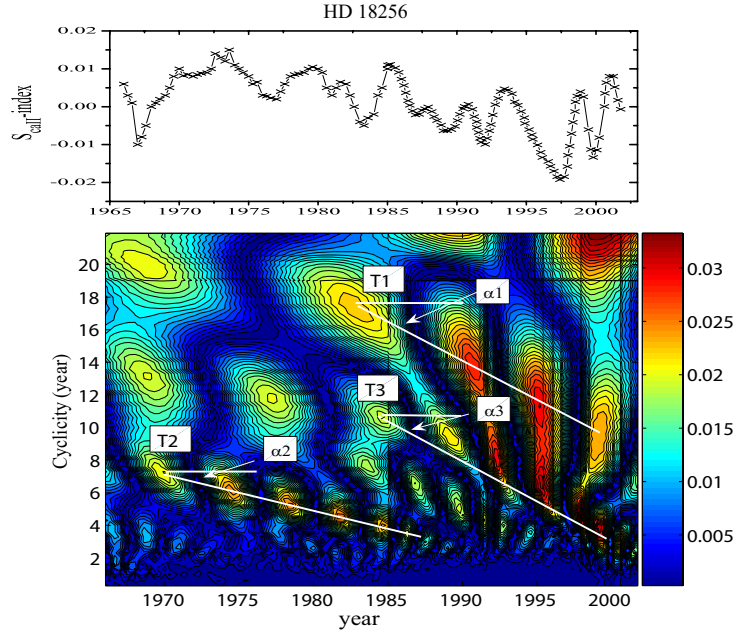
3.3 HK Project Stars in the "Fair" Class

In Figure 11 we show cycles of "Fair" class star HD 1835. We can see that observations made by Baliunas et al. (1995) during 1966–1985 and Lockwood et al. (2007) during 1985–2002 complement each other and there is an opportunity to identify the main longer cycle $T1$, that diminished from 22 to 19 yr from 1982 to 2002. We can also see the weaker cycle with a period of $T2$ (10.0 yr according to Baliunas et al. (1995)) which changed from 12 to 7.5 yr from 1975 to 1995.

In Figure 12 the cycles of "Fair" class star HD 18256 are displayed. It is apparent that observations by Baliunas et al. (1995) during 1966–1985 and by Lockwood et al. (2007) during 1985–2002 also complement each other. The main cycle $T1$ changes from 18 to 10 yr from 1983 to 2002. The second power period $T2$ (coinciding with the "Fair" class cycle in Baliunas et al. 1995 with 6.8 yr duration) changed from 7.5 to 4.5 yr from 1970 to 1977. In Figure 12 we can also see another weaker cycle with a period of $T3$ which changed from 11 yr to 4.5 yr from 1970 to 1987.
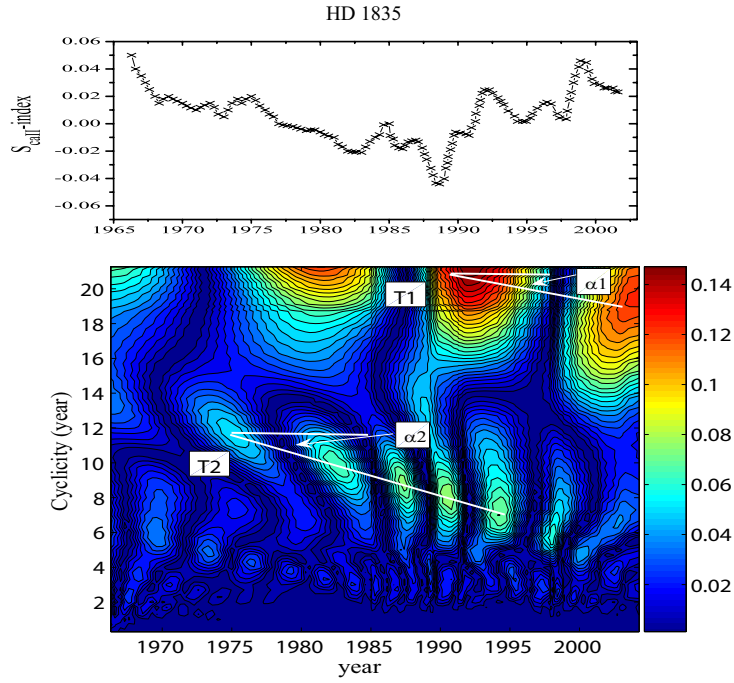
HD 1835

Fig. 11 Three-month averaged data of "Fair" class star HD 1835. Observations from 1966 to 2002 (*top panel*); Cyclic activity of HD 1835 (*bottom panel*). The *white lines* show temporal trends in the cycle's duration.
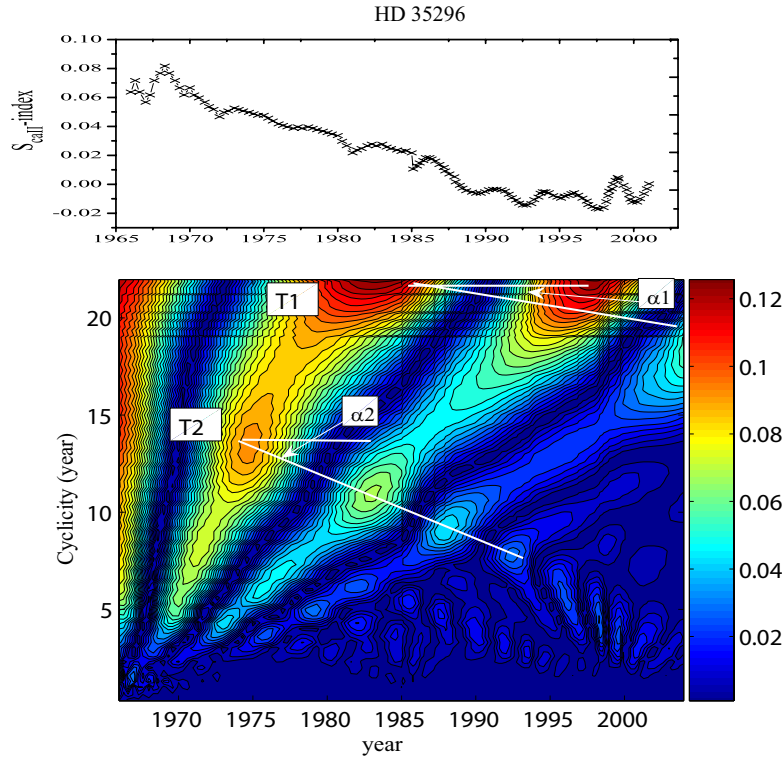
HD 18256

Fig. 12 Three-month averaged data of "Fair" class star HD 18256. Observations from 1966 to 2002 (*top panel*); Cyclic activity of HD 18256 (*bottom panel*). The *white lines* show temporal trends in the cycle's duration.

3.4 HK Project Stars in the "Long" Class

"Long" means significant variability on timescales longer than 25 yr.

In Figure 13 we show cycles of "Long" class star HD 35296. We used the long term set of observations which spans 36 yr. We found that the main long cycle $T1$ changes from 25 to 21 yr from 1975 to 2000. We can also see the weaker cycle with a period of $T2$ which changed from 14 to 7.5 yr from 1975 to 1994.
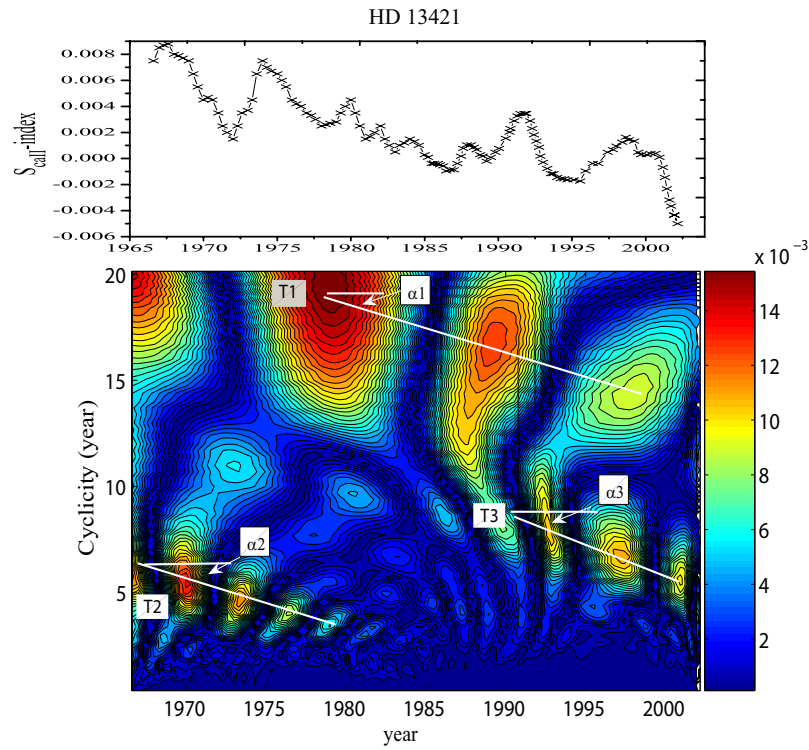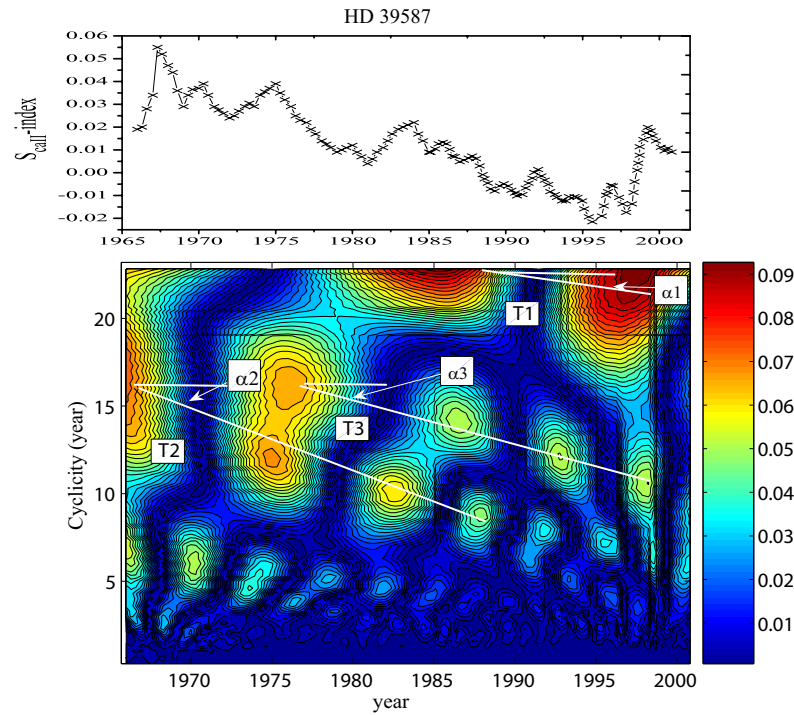
Fig. 13 Three-month average data of "Long" class star HD 35296. Observations from 1966 to 2002 (*top panel*); Cyclic activity of HD 35296 (*bottom panel*). The *white lines* show temporal trends in the cycle's duration.
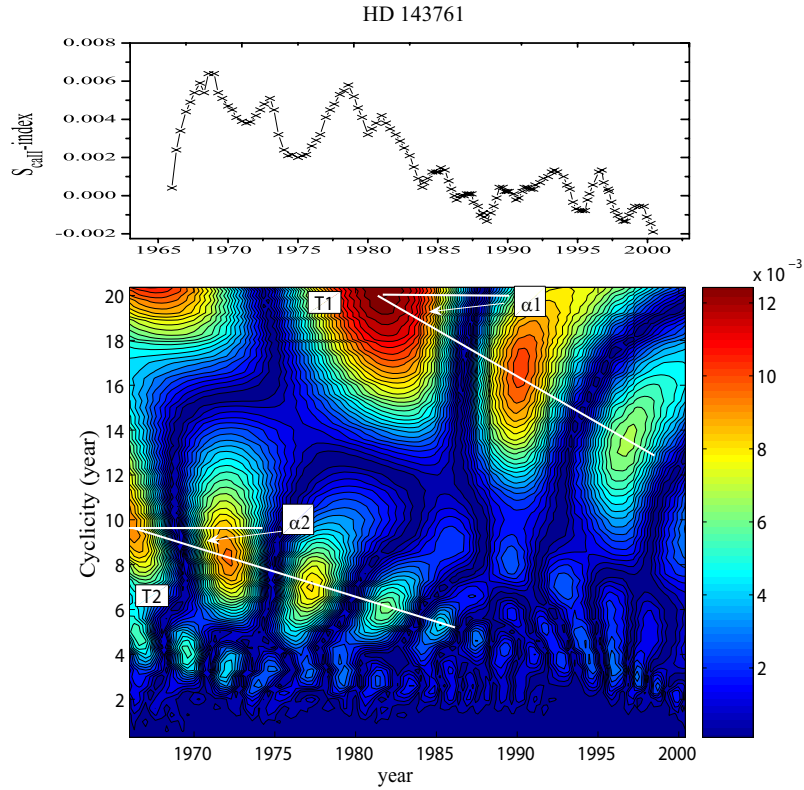
Fig. 14 Three-month averaged data of "Long" class star HD 143761. Observations from 1966 to 2002 (*top panel*); Cyclic activity of HD 143761 (*bottom panel*). The *white lines* show temporal trends in the cycle's duration.

Fig. 15 Three-month averaged data of "Flat" class star HD 13421. Observations from 1966 to 2002 (*top panel*); Cyclic activity of HD 13421 (*bottom panel*). The *white lines* show temporal trends in the cycle's duration.

Fig. 16 Three-month averaged data of "Var" class star HD 39587. Observations from 1966 to 2002 (*top panel*); Cyclic activity of HD 39587 (*bottom panel*). The *white lines* show temporal trends in the cycle's duration.

In Figure 14 we show cycles of "Long" class star HD 143761. We have also combined the observations of Baliunas et al. (1995) for 1966–1985 with observations of Lockwood et al. (2007). The main long cycle $T1$ changes from 24 to 17 yr from 1968 to 2000. We can also see the weaker cycle with a period of $T2$ which changed from 10 to 6 yr from 1966 to 1980.

3.5 HK Project Stars in the "Flat" Class

Stars in the "Flat" class mean that the average ratio of dispersion of S to the value of S ($\langle \sigma_S / S \rangle$) is less than 1%–1.5%.

In Figure 15 we show cycles of the "Flat" class star HD 13421. The combination of observations of Baliunas et al. (1995) from 1966–1985 with observations of Lockwood et al. (2007) helps us to find three cycles. The main long cycle $T1$ changes from 19 to 15 yrs from 1979 to 1999. We can also see the two weaker cycles with a period of $T2$ which changed from 6.5 to 4 yr from 1966 to 1979 and with a period of $T3$ which changed from 8 to 6 yr from 1991 to 2001.

3.6 HK Project Stars in the "Var" Class

Baliunas et al. (1995) classified stars as "Var" which are characterized by variability without pronounced periodicity on timescales longer than 1 yr but much shorter than 25 yr.

The average ratio of the dispersion of S to the S value for "Var" stars should be more than 2% ($\langle \sigma S / S \rangle) \geq 2\%$

In Figure 16 we show cycles of "Var" class star HD 39587. The combination of observations by Baliunas et al. (1995) during 1966–1985 with observations by Lockwood et al. (2007) helps us to find three cycles. The main long cycle $T1$ changes from 24 to 21 yr from 1985 to 2000. We can also see the two weaker cycles with a period of $T2$ which changed from 16 to 9 yr from 1966 to 1982 and with a period of $T3$ which changed from 16 to 10.5 yr from 1977 to 1999.

4 THE PARAMETERS OF THE TIME-EVOLUTION OF THE CYCLES

To describe this general trend we propose a formal representation of this process. The cyclic variations of fluxes of solar radiation and stellar radiation can be represented by the expression which describes the trends in the values of the periods of magnetic activity

$$Ti(t) = Ti^0 - (t - ti^0) \cdot tg\alpha i. \qquad (1)$$

In Table 1 we present the values of Ti for the Sun and HK Project stars with different cyclicity classes. We show the main (according to wavelet coefficient map) period in magnetic activity $T1$ and also the periods with lower power $T2$ and $T3$ in the case when we see the presence of multiple cyclicities.

For the determination of parameters of the cycle's time-evolution in cases of HK Project stars, we used the wavelet coefficient map calculated for these stars (Figs. 7–16) with $T1$–$T3$ and $\alpha 1 - \alpha 3$ values which are shown in these figures.

For the Sun, the period $T1$ ("11-yr" cycle) is shown in Figure 5. The period $T2$ ("100-yr" cycle) is displayed in Figure 2. The period $T3$ ("quasi-biennial" cycle) is exhibited in Figure 6.

5 CONCLUSIONS

(1) The problem of studying the evolution of cyclic activity in the Sun is very relevant at the present time. The close interconnection between activity indices enables new capabilities in the solar activity index forecasts. For these purposes successful forecasts of maximum values and other parameters in future activity cycles are necessary, which require taking the 11-yr and century components in solar cyclicity and their evolution into account in the simulation of processes in the Earth's ionosphere and upper atmosphere.

(2) Wavelet analysis allows detecting cycles among Sun-like stars based on observations of the S_{HK}-index which were previously considered as "Var," "Flat" and "Long." All the stars in our pattern are characterized by the presence of multiple cycles like the Sun (as was earlier found for 20 stars in Oláh et al. (2009)).

(3) Periods of solar and stellar cycles show gradual changes with time. Are the periods of the cycles gradually decreasing from maximum to minimum? Then there comes a moment when the duration of the cycle abruptly changes: the minimum value of a period sharply grows to the maximum value of this period. Sometimes we see a forked cycle, then the cyclicity with the minimum period disappears and the cycle begins to evolve again with a gradual de-

crease in the period value until the next sharp jump in the period from minimum to maximum.

References

Baliunas, S. L., Donahue, R. A., Soon, W. H., et al. 1995, ApJ, 438, 269

Bludova, N. G., Obridko, V. N., & Badalyan, O. G. 2014, Sol. Phys., 289, 1013

Bruevich, E. A., Katsova, M. M., & Sokolov, D. D. 2001, Astronomy Reports, 45, 718

Bruevich, E. A., & Alekseev, I. Y. 2007, Astrophysics, 50, 187

Bruevich, E. A., & Kononovich, E. V. 2011, Moscow University Physics Bulletin, 66, 72

Bruevich, E. A., Bruevich, V. V., & Yakunina, G. V. 2014, Sun and Geosphere, 8, 91

Bruevich, E. A., & Yakunina, G. V. 2015, Moscow University Physics Bulletin, 70, 282

Daubechies, I. 1990, IEEE Transactions on Information Theory, 36, 961

Frick, P., Baliunas, S. L., Galyagin, D., Sokoloff, D., & Soon, W. 1997, ApJ, 483, 426

García, R. A., Mathur, S., Salabert, D., et al. 2010, Science, 329, 1032

Kolláth, Z., & Oláh, K. 2009, A&A, 501, 695

Lockwood, G. W., Skiff, B. A., Henry, G. W., et al. 2007, ApJS, 171, 260

Metcalfe, T. S., Monteiro, M. J. P. F. G., Thompson, M. J., et al. 2010, ApJ, 723, 1583

Morgenthaler, A., Petit, P., Morin, J., et al. 2011, Astronomische Nachrichten, 332, 866

Nagovitsyn, Y. A., Tlatov, A. G., & Nagovitsyna, E. Y. 2016, Astronomy Reports, 60, 831

Noyes, R. W., Hartmann, L. W., Baliunas, S. L., Duncan, D. K., & Vaughan, A. H. 1984, ApJ, 279, 763

Oláh, K., Kolláth, Z., Granzer, T., et al. 2009, A&A, 501, 703

Scargle, J. D. 1982, ApJ, 263, 835

Shimanovskaya, E., Bruevich, V., & Bruevich, E. 2016, RAA (Research in Astronomy and Astrophysics), 16, 148

Svalgaard, L., Lockwood, M., & Beer, J. 2011, Long-term reconstruction of Solar and Solar Wind Parameters, *http://www.leif.org/research/Svalgaard_ISSI_Proposal_Base.pdf*.

Vaughan, A. H., & Preston, G. W. 1980, PASP, 92, 385

Vitinskij, Y. I., Kopetskij, M., & Kuklin, G. V. 1986, Statistics of the Spot-forming Activity of the Sun (Nauka, Moskva. In Russian)

Zhao, J.-K., Oswalt, T. D., Chen, Y.-Q., et al. 2015, RAA (Research in Astronomy and Astrophysics), 15, 1282